

THE UNIVERSITY OF MICHIGAN  
INDUSTRY PROGRAM OF THE COLLEGE OF ENGINEERING

TRANSIENT PHENOMENA ASSOCIATED WITH THE PRESSURIZATION OF  
LIQUID NITROGEN BOILING AT CONSTANT HEAT FLUX



S. K. Fenster  
G. J. Van Wylene  
J. A. Clark

October, 1959

IP-396

Engn  
UMR  
1422

## INTRODUCTION

This investigation concerns liquid nitrogen which is boiling as a result of a constant heat flux through the walls of the containing vessel. When this boiling liquid is pressurized, boiling ceases because the fluid is now sub-cooled with respect to the new saturation temperature. A transient process then follows in which the liquid is heated and boiling initiated. Finally steady state boiling at the new saturation temperature is achieved.

The purpose of this investigation was to study the transient phenomena following pressurization. The transient heat transfer coefficients in the liquid nitrogen have been calculated from experimental data and an analytical study made.

## EXPERIMENTAL APPARATUS

Because this study is relevant to the pressurization of the liquid oxygen tanks of missiles, the length to diameter ratio, wall thickness, and materials of the primary test cylinder were influenced by actual missile practice. The apparatus consisted essentially of a cylinder three feet high and one foot in diameter which contained liquid nitrogen. The heat flux through the container walls could be regulated and measured. Temperature at various wall heights and throughout the liquid were measured as a function of time by use of thermocouples. The flux was varied from 1000 to 4000 BTU/hr ft<sup>2</sup> and pressurizations to 20 and 35 psig were used. The rate of vapor boiloff was also measured. A guard heater was used to insure that accurate measurements of heat input were obtained. Figures 1 and 2 give details of the apparatus and test layout.

## EXPERIMENTAL RESULTS

Immediately upon pressurization of the liquid nitrogen boiling at atmospheric pressure, boiling ceases and the wall and liquid undergo temperature transients. Figures 3 and 5 show characteristic data for two runs having different heat fluxes, but the same level of pressurization. From the defining equations,

$$h = \frac{(q/A)}{t_{WX} - t_{LX}} \quad (1)$$

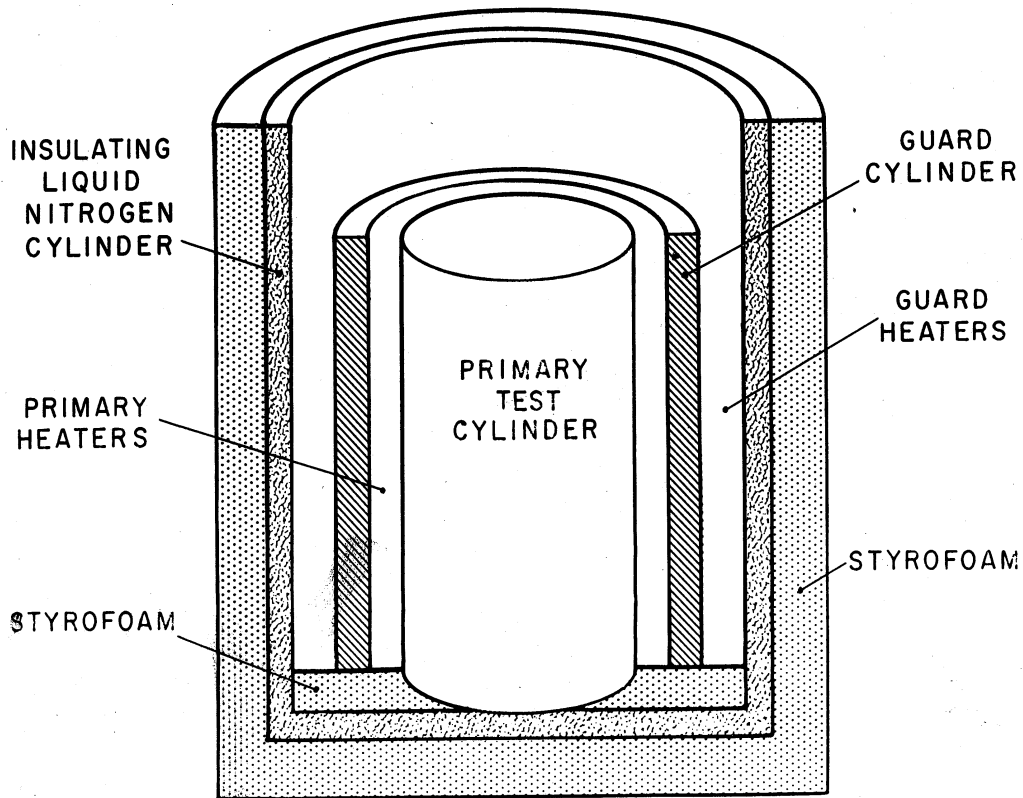


Figure 1. Test Assembly.

the heat transfer coefficient may be calculated for several locations. The liquid temperatures were found to be, within the limits of experimental accuracy, independent of radial location. This is to be expected since no liquid temperatures were measured close to the wall.

The transient heat transfer coefficients, shown in Figures 4 and 6 correspond respectively to the data given in Figures 3 and 5.

By defining dimensionless temperature and time ratios, the liquid temperature transients for all the tests were reduced to a single curve for each longitudinal location. As the ordinate,  $\theta/\theta^*$ , was used, where  $\theta$  is the instantaneous temperature of the liquid above the saturation temperature:

$$\theta = t_{Lx} - t_{l \text{ sat.}} \quad (2)$$

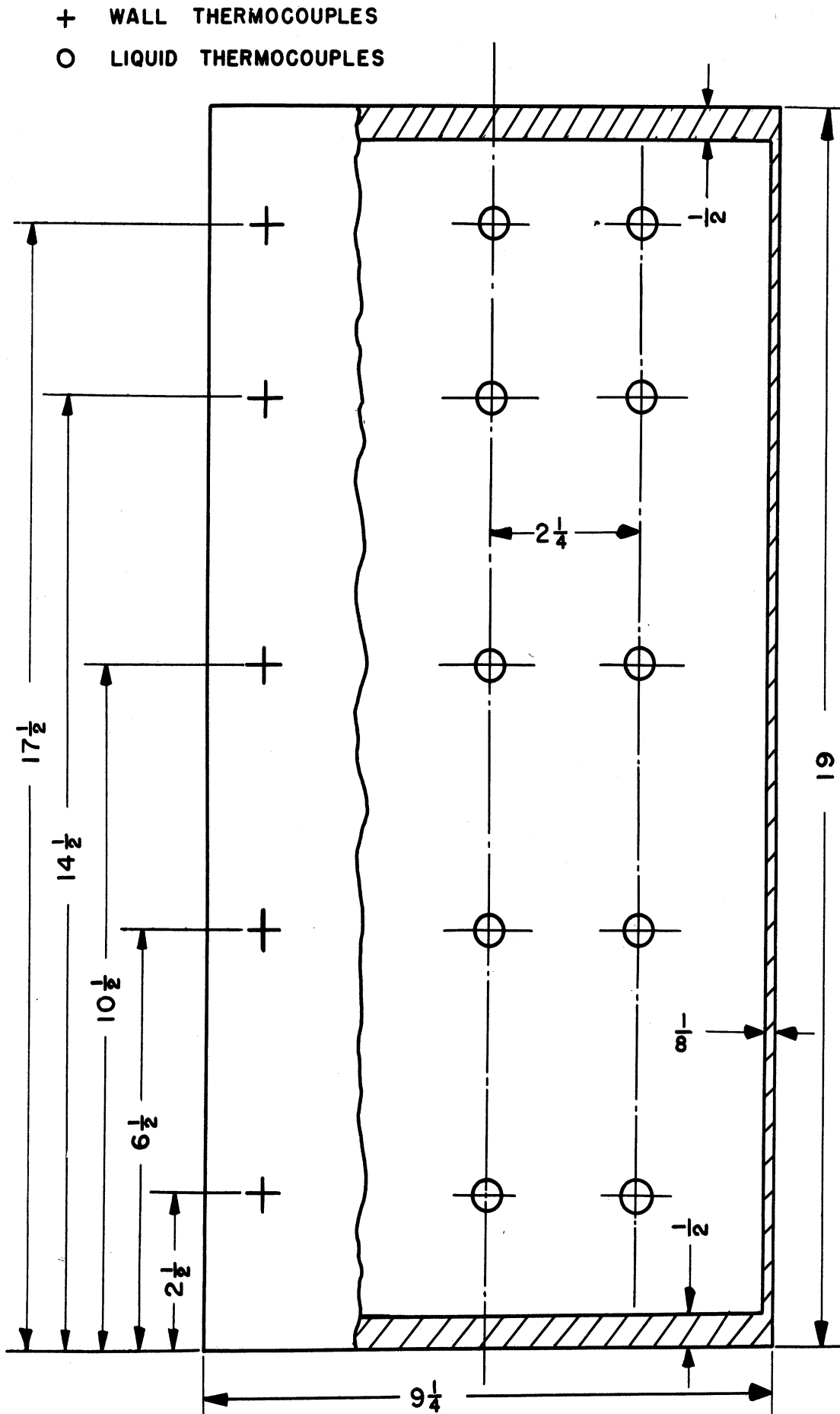


Figure 2. Basic Test Cylinder Dimensions and Thermocouple Locations.

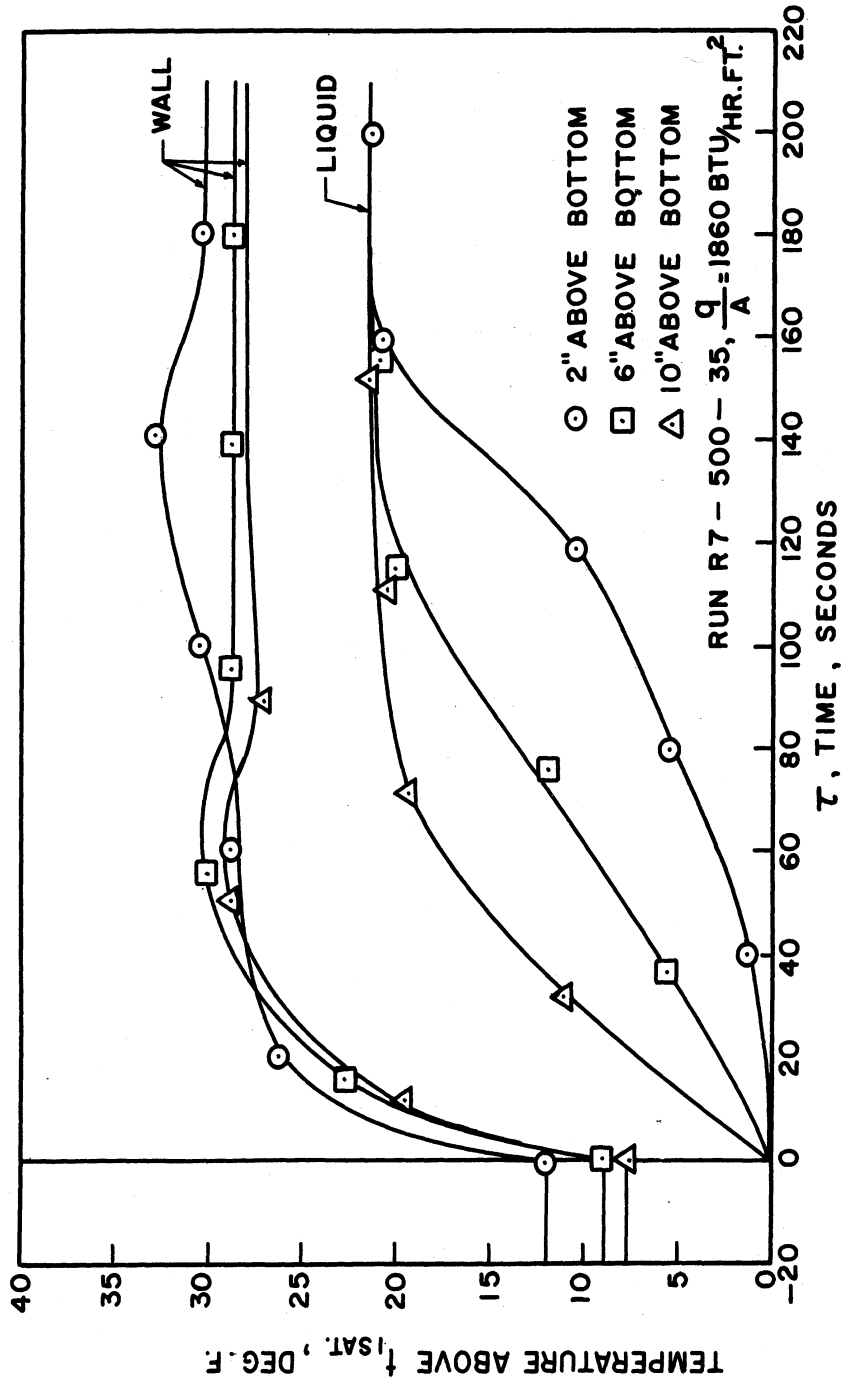


Figure 3. Wall and Liquid Temperatures vs. Time, Run R7-500-35.

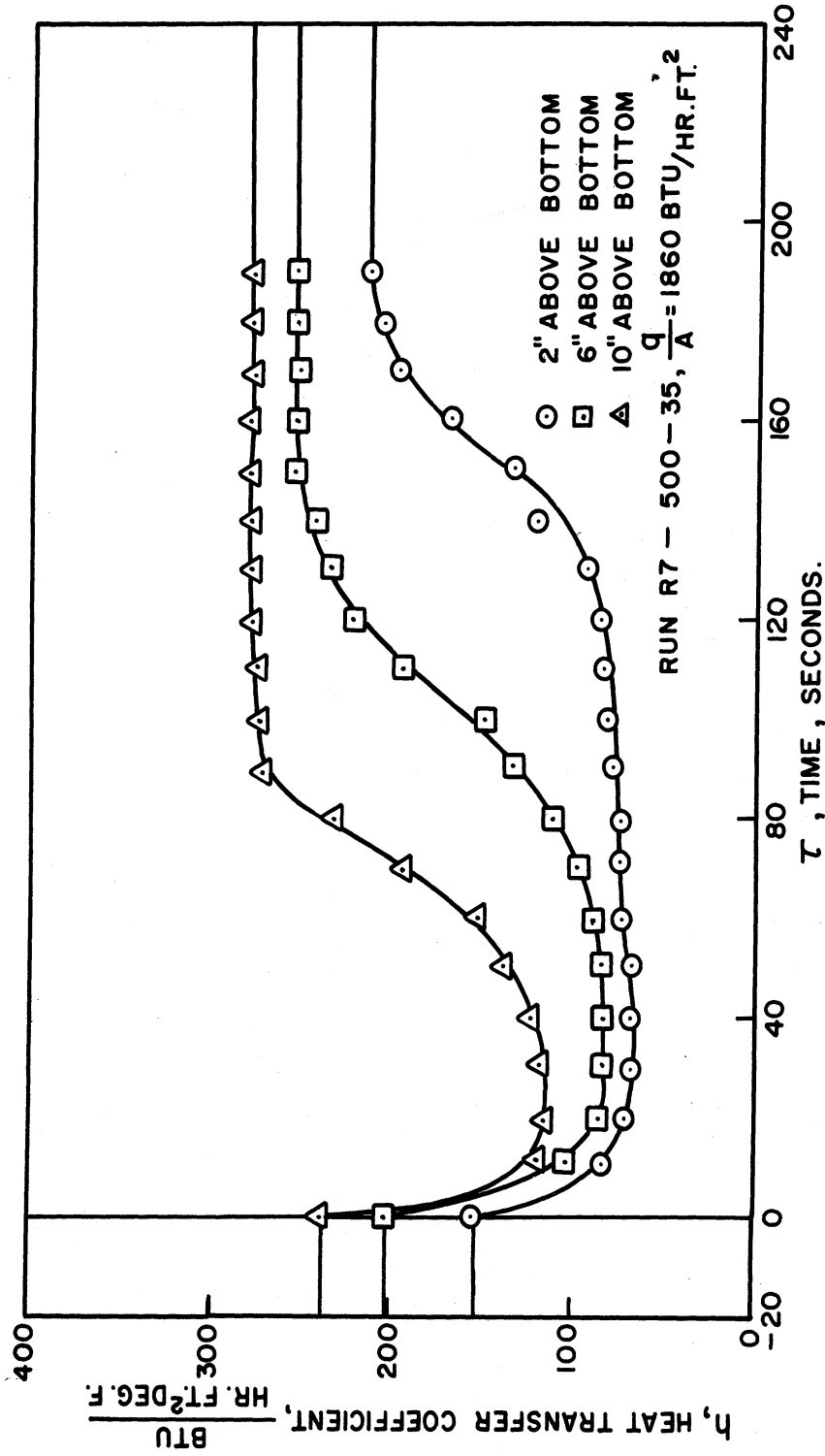


Figure 4. Heat Transfer Coefficient vs. Time, Run R7-500-35.

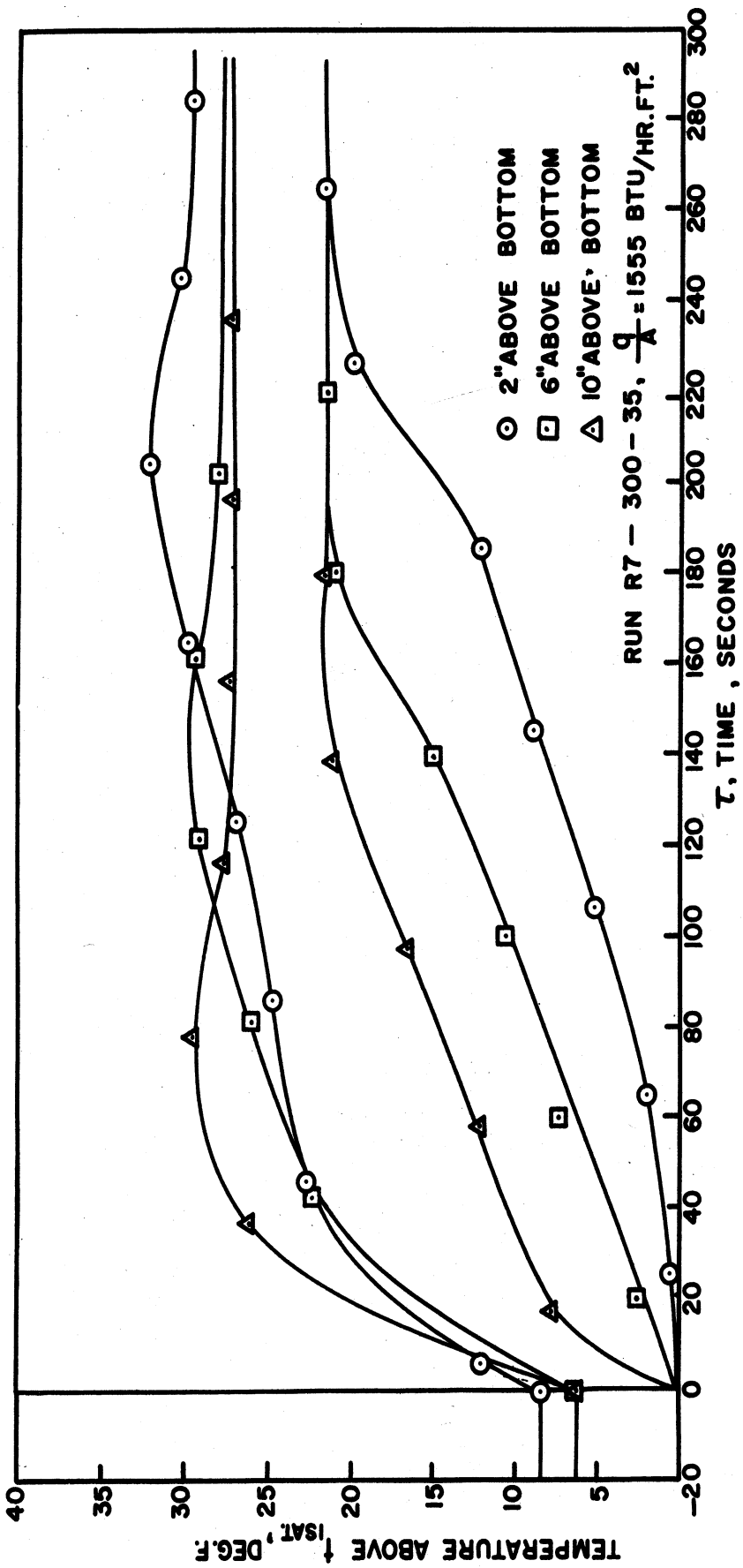


Figure 5 Wall and Liquid Temperatures vs. Time, Run R7-300-35.



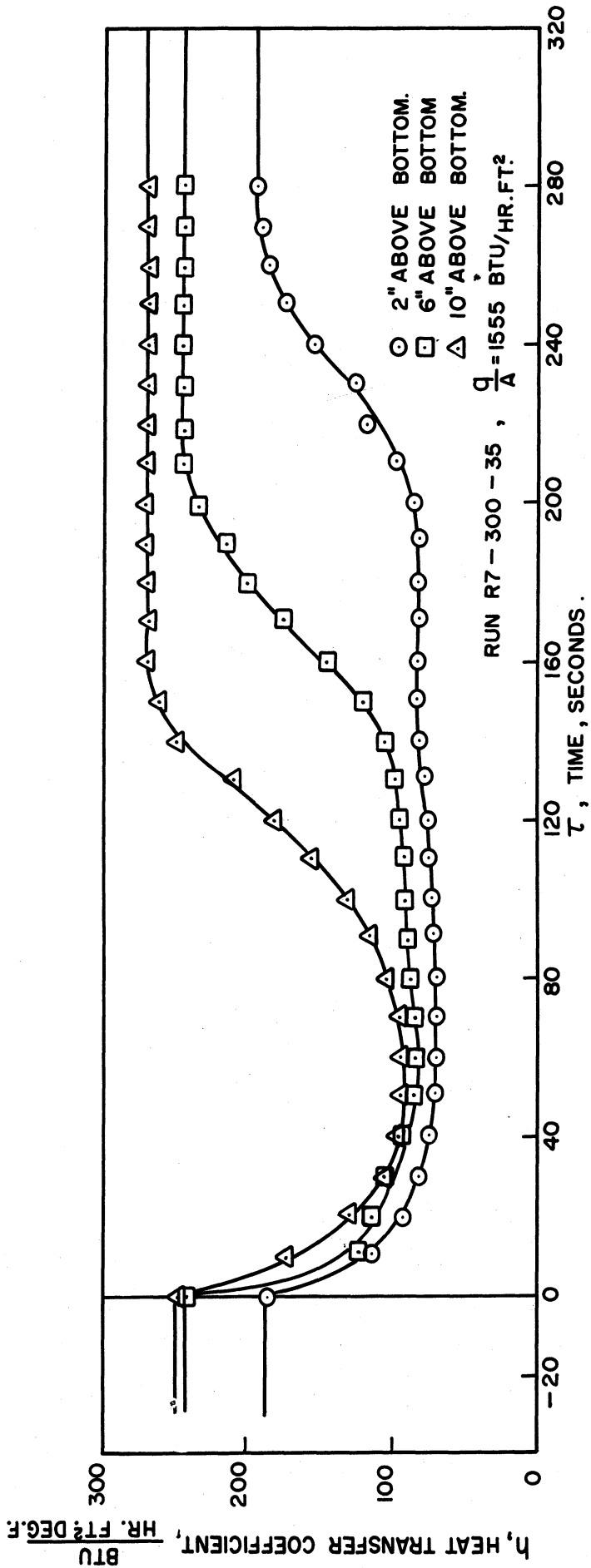


Figure 6. Heat Transfer Coefficient vs. Time, Run R7-300-35.

$\theta^*$  is defined as the difference between the final and initial saturation temperatures:

$$\theta^* = t_2 \text{ sat.} - t_1 \text{ sat.} \quad (3)$$

As the abscissa, a dimensionless time,  $\tau/\tau^*$ , is used.  $\tau$  is the time interval after pressurization.  $\tau^*$  represents the calculated time required for the mass of liquid nitrogen under test to be heated from its initial to its final saturation temperature at the prescribed heat flux, assuming no boiling occurs anywhere in the system:

$$\tau^* = \frac{W_L C_{pL} (t_2 \text{ sat.} - t_1 \text{ sat.})}{(q/A)A} = \frac{W_L C_{pL} \theta^*}{q} \quad (4)$$

The results of this dimensionless plot are shown in Figure 7.

The steep wall temperature transients immediately upon pressurization are to be expected because the heat transfer coefficient decreases significantly when boiling ceases. Since the quantity of heat passing through the outer primary cylinder wall is constant, the wall temperature must rise. However, the wall temperatures level off because a steady state equilibrium is established between the heat flux, and wall and liquid temperatures.

#### TIME VARIATION OF THE HEAT TRANSFER COEFFICIENT

The transient heat transfer coefficient as shown in Figures 4 and 6 is characterized by a rapid decrease following pressurization, a minimum point or dwell period, the duration of which depends on the longitudinal location and flux, and finally a rapid increase until steady state boiling is reestablished. A qualitative explanation of this phenomenon follows:

During steady state boiling, the coefficient at a given longitudinal position remains constant. Upon pressurization the bubbles collapse, and the agitation associated with the bubble formation and escape ceases. The forces then acting to influence the heat transfer coefficient after pressurization are as follows:

(1) Viscous forces which tend to decelerate the fluid and hence decrease the coefficient.

(2) Free convection (the term "free convection" is used to describe the component of the fluid motion due to temperature difference between the wall and the liquid) tending to increase the coefficient during that period in which the difference in temperature between the wall and liquid is increasing.

(3) Some time after pressurization bubbles begin to form and this tends to increase the heat transfer coefficient.

A quantitative approach to the heat transfer coefficient transient during that period from pressurization to the point at which the coefficient reaches a minimum point or dwell, is based upon the fact that the Reynolds number represents the ratio of inertia forces to viscous forces. The following Reynolds number is defined:

$$Re = \frac{\rho_L u L}{\mu_f} = \frac{u L}{\nu_f} = \frac{L^2}{\tau \nu_f} \quad (5)$$

The following expression for the decay of the heat transfer coefficient due to viscous deceleration is postulated:

$$\frac{\Delta h}{\Delta h_0} = e^{-\frac{C_2}{Re}} = e^{-\frac{C_2 \nu_f \tau}{L^2}} \quad (6)$$

In other words, the heat transfer coefficient diminishes through viscous decay following an equation typical of first order effects. The quantities involved in Equation (6) have had the free convection effect subtracted out thus leaving the viscous terms only.

The justification of these expressions is based on the supposition that in that period after pressurization only the first two factors cited above (that is, the viscous decay and free convection) influence the heat transfer coefficient, and that no bubbles have formed during this period. The reasons for believing this to be a reasonable assumption are as follows:

(1) When pressurization occurs, the rate of decrease of the heat transfer coefficient is very rapid because the primary cause of fluid motion, namely, bubble formation and escape, no longer exist. It is assumed that the increase in the heat transfer coefficient which takes place after the minimum period is due to the reinitiation of boiling. Therefore, until this increase takes place it may reasonably be assumed that there is no boiling.

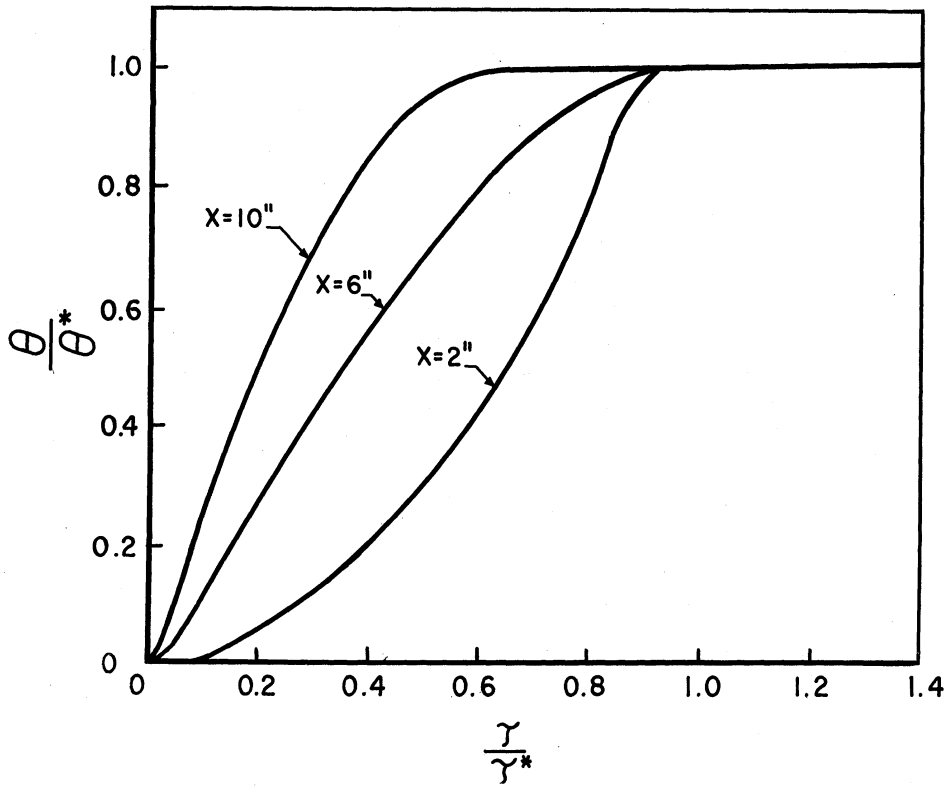


Figure 7. Dimensionless Liquid Temperature vs. Dimensionless Time.

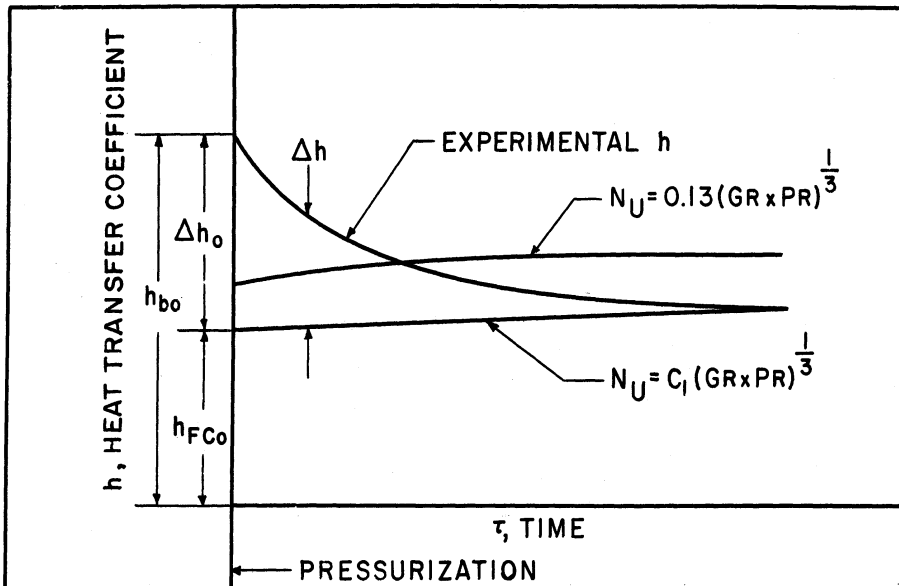


Figure 8. Curves Showing Definition of  $\Delta h$  and  $\Delta h_0$ .

(2) For a certain period after pressurization the wall temperatures are below the new saturation temperature and therefore no bubbles can form. Furthermore, a certain amount of superheat in the liquid at the wall is necessary before boiling can be reinitiated, but less superheat is needed to maintain boiling. The maximum wall temperature which is observed in Figures 3 and 5 is believed to be associated with that point at which boiling is reinitiated.

Therefore it is reasonable to assume that until the time of the minimum heat transfer coefficient, the only driving force tending to increase the coefficient is the temperature difference between the wall and the liquid. Furthermore, it will be assumed that at this minimum point, viscous deceleration is essentially complete and the heat transfer coefficient is due entirely to the buoyant forces associated with free convection.

The correlation used for turbulent free convection from vertical surfaces, sometimes called the Jakob correlation<sup>(1)</sup> is as follows:

$$Nu = 0.13 (Gr \cdot Pr)^{1/3} \quad (7)$$

If the heat transfer coefficient for turbulent free convection is calculated using the above relationship and drawn as a function of time on the same graph as the experimentally obtained heat transfer coefficients, a result similar to that shown in Figure 8 is obtained. It is evident that this correlation gives values which are too high. However, the correct correlation for the heat transfer coefficient at the minimum point can be obtained by assuming that the exponent in the Jakob correlation is the same, but the coefficient for the equation is changed. This is a reasonable result since the reason there is any difference to begin with is attributable to the stagnant zone which necessarily exists at the bottom of the test vessel. Several workers<sup>(2,3,4)</sup> have also noted that the coefficient of heat transfer for closed end cylinders is substantially less than that for plane vertical surfaces or outside of vertical tubes. Table I gives the results described above.

When this new equation is used for free convection, the free convection term can be subtracted from the total heat transfer coefficient, and the fraction  $\Delta h / \Delta h_0$  calculated. For low heat flux runs Figure 9 represents a plot of  $\Delta h / \Delta h_0$  vs. dimensionless time. The equation for the line drawn through these points is:

$$\frac{\Delta h}{\Delta h_0} = e^{-0.892 \times 10^5 \frac{v_f \tau}{L^2}} \quad (8)$$

TABLE I

COMPARISON OF MINIMUM HEAT TRANSFER COEFFICIENTS  
WITH VALUES COMPUTED USING CORRELATION FOR  
VERTICAL SURFACES IN TURBULENT FLOW

Heat Flux BTU/hr ft <sup>2</sup> /Final gage pressure, psi	h <sub>min</sub> /h <sub>FC</sub>		
	x = 2 in.	x = 6 in.	x = 10 in.
1860/20	0.55	0.67	0.85
1780/35	0.48	0.53	0.62
2040/35	0.48	0.58	0.97
1555/35	0.47	0.60	0.68
1860/35	0.44	0.55	0.88
1470/20	0.54	0.61	0.64
Mean	0.49	0.59	0.77

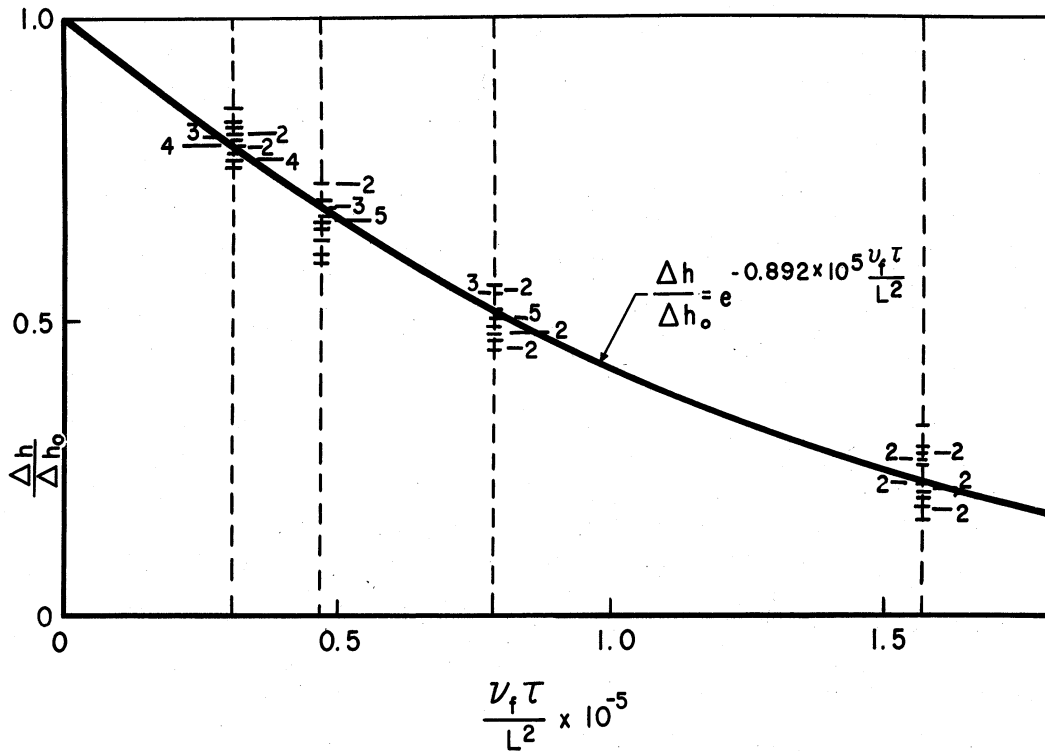


Figure 9. Viscous Attenuation of the Heat Transfer Coefficient.

The form of the equation, indicative of a first order effect, indicates that when the effect of free convection is subtracted from the total heat transfer coefficient, the remaining transient shows essentially the effect of viscous decay only.

### CONCLUSIONS

The coefficient of heat transfer following pressurization up to the time of first bubble formation is therefore expressed as the sum of two terms. The first relates to the free convection contribution, the second to the viscous diminution of the initial turbulence:

$$\frac{h_L}{k_L} = C_1 (Gr \cdot Pr)^{1/3} + \frac{\Delta h_0 L}{k_L} e^{-\frac{C_2 V_f \tau}{L^2}} \quad (9)$$

### REFERENCES

1. Jakob, M. Heat Transfer. I. New York: John Wiley and Sons, (1955), 529-530.
2. Eckert, E. R. G., and Diaguila, A. J. "Experimental Investigation of Free Convection Heat Transfer in Vertical Tube at Large Grashof Numbers." NACA, Report 1211, 1955.
3. Hartnett, J. P., and Welsh, W. E. "Experimental Studies of Free Convection Heat Transfer in Vertical Tube with Uniform Wall Heat Flux." Trans. ASME, 79, (1957), 551-556.
4. Siegel, R., and Norris, R. H. "Tests of Free Convection in a Partially Enclosed Space between Two Heated Vertical Plates." Trans. ASME, 79, (1957), 663-670.

### NOMENCLATURE

- $C_1$  See Equation (9)
- $C_2$  See Equation (6)
- $c_{pL}$  Specific Heat of Liquid

Gr	Grashof number, $\beta_L \Delta T g \rho_L^2 x^3 / \mu_f^2$
g	Gravitational Acceleration
h	Heat Transfer Coefficient
$h_{bo}$	Boiling Heat Transfer Coefficient at Time Zero
$h_{FC}$	Free Convection Heat Transfer Coefficient
$h_{FCo}$	Free Convection Heat Transfer Coefficient at Time Zero
$\Delta h$	$h - h_{FC}$
$\Delta h_o$	$h_{bo} - h_{FCo}$
$k_L$	Thermal Conductivity of Liquid
L	Liquid Level
Nu	Nusselt Number, $hL/k_L$
Pr	Prandtl Number, $c_{pL} \mu_f / k_L$
q	Heat Rate
(q/A)	Heat Flux
Re	Reynolds Number, see Equation (5)
$t_{1 \text{ sat.}}$	Saturation Temperature of Liquid at Initial Pressure
$t_{2 \text{ sat.}}$	Saturation Temperature of Liquid at Final Pressure
$t_{wx}$	Wall Temperature at Longitudinal Location x
$t_{Lx}$	Liquid Temperature at Longitudinal Location x
$\Delta T$	Wall-Liquid Temperature Difference
u	Velocity, see Equation (5)
$w_L$	Mass of Liquid Under Test



x	Coordinate, Measured Upward from Test Cylinder Bottom
$\beta_L$	Volumetric Coefficient of Expansion of Liquid
$\theta$	$t_{Lx} - t_1 \text{ sat.}$
$\theta^*$	$t_2 \text{ sat.} - t_1 \text{ sat.}$
$\mu_f$	Absolute Viscosity of Liquid
$\nu_f$	Kinematic Viscosity of Liquid
$\rho_L$	Liquid Density
$\tau$	Time
$\tau^*$	See Equation (4)

UNIVERSITY OF MICHIGAN



3 9015 02826 7808